Competitive Double Diffusive Convection in a Kelvin–Voigt Fluid of Order One

Brian Straughan[1]

Abstract

We present a model for convection in a Kelvin–Voigt fluid of order one when the layer is heated from below and simultaneously salted from below, a problem of competitive double diffusion since heating from below promotes instability, but salting from below is stabilizing. The instability surface threshold is calculated and this has a complex shape. The Kelvin–Voigt parameters play an important role in acting as stabilizing agents when the convection is of oscillatory type. Quantitative values of the instability surface are displayed. The nonlinear stability problem is briefly addressed.

1 Introduction

The classes of fluids being employed or discovered in geophysical and industrial engineering applications is increasingly diverse. Many fluids are now highly complex and are not adequately described by a stess tensor which depends linearly on the velocity gradient. Complex fluids are those which include viscoelastic fluids where the stress tensor depends on the history of the velocity gradient, and nanofluid suspensions, cf. Haavisto et al. [1], which involve a suspension of extremely fine particles in a carrier fluid. Such a suspension may require dependence on second gradients of the velocity field to incorporate physical effects such as the flattening of the parabolic profile of Poiseuille flow, cf. Straughan [2]. The field of viscoelastic fluids which includes fading memory fluids is vast, as is witnessed by the work of Amendola and Fabrizio [3], Amendola et al. [4], Anand et al. [5], Anand and Christov [6,7], Anh and Nguyet [8], Christov and Christov [9], Fabrizio et al. [10], Franchi et al. [11–14], Gatti et al.

✉ Brian Straughan
brian.straughan@durham.ac.uk

[1] Department of Mathematical Sciences, University of Durham, Stockton Road, Durham DH1 3LE, UK

[15], Jordan et al. [16], Jordan and Puri [17], Payne and Straughan [18], Yang et al. [19].

In this article we concentrate on a particular class of viscoelastic fluids associated with the names of Kelvin and of Voigt, cf. Avalos et al. [20], Anh and Nguyet [8], Chirita and Zampoli [21], El Arwadi and Youssef [22], Layton and Rebholz [23], Rivera and Racke [24]. Analytical studies of Kelvin–Voigt fluids have been presented by Oskolkov [25,26], and generalizations of these to to incorporate temperature effects are given by Sukacheva and Matveeva [27], Matveeva [28] and Sukacheva and Kondyukov [29]. The general complex relationship between the stress and the history of the velocity gradient in a viscolelastic fluid is often approximated by including time derivatives of the stress and/or velocity gradient of various orders. These typically result in what are known as Maxwell fluids, Oldroyd fluids, or Kelvin–Voigt fluids. A very useful account of Maxwell, Oldroyd and Kelvin–Voigt fluids of various orders is given by Oskolkov and Shadiev [30] who discuss the solution existence question at length, cf. also Christov and Jordan [31].

Double diffusive convection involves the motion of a fluid (Newtonian or viscoelastic) wherein a salt is dissolved in the fluid and temperature effects are considered. This phenomenon is widely studied in the literature, see e.g. Barletta and Nield [32], Capone et al. [33], Galdi et al. [34], Gentile and Straughan [35], Harfash and Hill [36], Nield [37], Matta et al. [38], Mulone [39], Payne et al. [40], Straughan [41–43], Straughan [44], chapter 12, Straughan and Hutter [45]. We here present an analysis for a double diffusion problem in a Kelvin–Voigt fluid of order one. We believe this is the first presentation and analysis of this problem. We refer to the phenomenon of competitive double diffusion because we treat instability in a fluid layer which is heated from below while simultaneously subject to a heavier salt concentration below. These two physical effects are opposing and lead to interesting mathematics and physics even for a Newtonian fluid. The double diffusion problem just described is called the thermosolutal convection or solar pond problem. When the convection Rayleigh number is increased the instability Rayleigh number boundary also increases, see e.g. Joseph [46], Mulone [39], Straughan [47]. However, for a Kelvin–Voigt fluid of order one the viscoelastic term in the momentum equation also has the effect of increasing the critical instability Rayleigh number as the appropriate viscoelastic coefficient is increased. Thus, we have two physical effects which each separately increase the Rayleigh number threshold for the onset of convective motion. When both effects increase the critical Rayleigh number, one may naively expect the additive effect to increase it further. For a Newtonian fluid the effects of rotation and a vertical magnetic field each separately increase the critical Rayleigh number, Chandrasekhar [48], figure 29, p. 121, and figures 39 and 43, pages 171 and 191. However, when both effects are combined the result is not one of each being additive and having an enhanced increasing effect, see Chandrasekhar [48], figure 47, p. 203. Therefore, one has to be careful and the problem of thermosolutal convection in a Kelvin–Voigt fluid of order one as analysed here leads to a complex array of behaviours.

We now present the equations of thermal and salt convection in a Kelvin–Voigt fluid of order one. We have not seen these presented before. After that we derive a detailed linear instability analysis and global nonlinear stability analysis for these equations.

2 Kelvin–Voigt Order One Equations

We now denote by $\mathbf{v}(\mathbf{x}, t)$, $T(\mathbf{x}, t)$, $C(\mathbf{x}, t)$, $p(\mathbf{x}, t)$ the velocity, temperature, concentration of a dissolved solute, and pressure at position $\mathbf{x}$ and time t of a body of fluid. When this fluid is of Kelvin–Voigt order one then the governing equations may be taken to be, Sukacheva and Matveeva [27], Straughan [47],

$$
\begin{aligned}
&(1 - \hat{\lambda}\Delta)v_{i,t} + v_j v_{i,j} = -\frac{1}{\rho_0} p_{,i} + \nu \Delta v_i + \alpha T g k_i - \zeta C g k_i + \hat{\beta}\Delta W_i \,, \\
&v_{i,i} = 0, \\
&T_{,t} + v_i T_{,i} = \kappa \Delta T \,, \\
&C_{,t} + v_i C_{,i} = \kappa_s \Delta C \,, \\
&W_{i,t} + \hat{\gamma} W_i = v_i \,,
\end{aligned}
\tag{1}
$$

where W_i is a viscoelastic variable defined by $(1)_5$. In addition $\hat{\lambda}$, ρ_0, ν, α, ζ, g, $\hat{\beta}$, κ, κ_s and $\hat{\gamma}$ are, respectively, the Kelvin–Voigt coefficient, a reference density, the kinematic viscosity, the coefficient of thermal expansion of the fluid, the expansion coefficient due to the solute, gravity, the viscoelastic coefficient in the momentum equation, thermal diffusivity, solute diffusivity, and the strength of viscoelasticity coefficient in the definition of W_i. The symbol Δ denotes the Laplacian, $\mathbf{k} = (0, 0, 1)$, gravity acts downward, and the body force term in $(1)_1$ arises from a Boussinesq approximation employing the density

$$
\rho = \rho_0[1 - \alpha(T - T_0) + \zeta(C - C_0)]
$$

for reference temperature and concentration, T_0, C_0, cf. the procedure in Straughan [49], section 14.1, Straughan [44], chapter 12.

We employ standard indicial notation throughout together with the Einstein summation convention. For example, the divergence of the velocity field is

$$
\begin{aligned}
v_{i,i} \equiv \sum_{i=1}^{3} v_{i,i} &= \frac{\partial v_1}{\partial x_1} + \frac{\partial v_2}{\partial x_2} + \frac{\partial v_3}{\partial x_3} \\
&= \frac{\partial u}{\partial x} + \frac{\partial v}{\partial y} + \frac{\partial w}{\partial z}
\end{aligned}
$$

where $\mathbf{v} = (v_1, v_2, v_3) \equiv (u, v, w)$ and $\mathbf{x} = (x_1, x_2, x_3) \equiv (x, y, z)$. A further example is

$$
v_i C_{,i} \equiv \sum_{i=1}^{3} v_i C_{,i} = u\frac{\partial C}{\partial x} + v\frac{\partial C}{\partial y} + w\frac{\partial C}{\partial z}.
$$

The Kelvin–Voigt terms, involving $\hat{\lambda}$ and $\hat{\beta}$ arise from a constitutive theory of form

$$\sigma_{ij} = \kappa_3 \frac{\partial d_{ij}}{\partial t} + 2\mu d_{ij} + \xi_1 \int_{-\infty}^{t} \exp\{-\hat{\gamma}(t-s)\} d_{ij} \, ds, \tag{2}$$

where $d_{ij} = (v_{i,j} + v_{j,i})/2$, $\mu = \rho_0 \nu > 0$ is the dynamic viscosity, and σ_{ij} is the Cauchy extra stress tensor, as shown by Oskolkov [25,26]. In fact, σ_{ij} is related to the stress tensor t_{ij} by $t_{ij} = -p\delta_{ij} + \sigma_{ij}$ and equation $(1)_1$ arises from the linear momentum equation

$$\rho_0(v_{i,t} + v_j v_{i,j}) = t_{ji,j} + \rho_0 f_i \,,$$

where f_i is the body force. To see this observe equation $(1)_5$ may be integrated with an integrating factor to deduce, recalling the fading memory effect, $W_i = \int_{-\infty}^{t} \exp\{-\hat{\gamma}(t-s)\} v_i \, ds$. The coefficients κ_3 and ξ_1 have form $\kappa_3 = 2\hat{\lambda}\rho_0$ and $\xi_1 = 2\hat{\beta}\rho_0$. It is noteworthy that the Kelvin–Voigt order one theory contains two extra parameters ξ_1 and $\hat{\gamma}$ which are not present in the Kelvin–Voigt order zero theory (also known as Navier–Stokes–Voigt theory), cf. Straughan [47], and these extra parameters yield a more accurate fit to experiments and provide a more refined fit to the fading memory behaviour, see e.g. Greco and Marano [50]. One should perhaps consider an objective derivative in (2), as is discussed in another context by Christov [51], cf. also Jordan et al. [52], equation (5b). However, in this article we follow the procedure of Sukacheva and Matveeva [27] and Sukacheva and Kondyukov [29].

It is important to observe that Kelvin–Voigt theory is being employed in various industrial and engineering applications to describe real materials. Gidde and Pawar [53] employ this theory to describe polydimethylsiloxane in a micropump, Jayabal et al. [54] use it to model skin in the context of the cosmetics industry, and Jozwiak et al. [55] employ Kelvin–Voigt fluids in their work on the dynamic behaviour of biopolymer materials. Erdel et al. [56] employ the complex shear moduli of a Kelvin–Voigt fluid model to calculate time-dependent coefficients for anomalous diffusion in a living cell nucleus. Askarian et al. [57] employ Kelvin–Voigt fluid models for the foundation for pipes conveying fluid. An important use of Kelvin–Voigt fluids is in the field of viscous dampers which are employed to reduce the effects of vibrations in large civil engineering structures, see e.g. Greco and Marano [50], Lewandowski and Chorazyczewski [58], Xu et al. [59]. In particular, high structures require viscous dampers, such as in the tower Taipei 101 in the city of Taipei. This tower is 1667 feet high and is very close to a fault line in the Earth's crust and it has been constructed to withstand typhoons and earthquakes. To make this possible Taipei 101 employs a 730 ton mass damper which is connected to eight viscous fluid dampers which act like shock absorbers when the mass damper moves.

3 Double Diffusive Convection

We shall suppose the Kelvin–Voigt order one fluid occupies the horizontal layer $0 < z < d$ where gravity is acting downward. Equations (1) are defined on the spatial region $\mathbb{R}^2 \times \{z \in (0,d)\}$, for $t > 0$.

The boundary conditions on the planes $z = 0$ and $z = d$ are given by

$$v_i = 0, \quad W_i = 0, \quad z = 0, d;$$
$$T = T_L, \quad z = 0, \quad T = T_U, \quad z = d; \tag{3}$$
$$C = C_L, \quad z = 0, \quad C = C_U, \quad z = d;$$

for prescribed constant values T_L, T_U, C_L, C_U, with $T_L > T_U > 0$ and $C_L > C_U$ where T_L, T_U are in °K. Thus, we analyse the interesting problem where the layer is hotter below which physically causes the fluid to expand and rise upward, whereas the layer is saltier below which causes the layer to be stable. The competition between these two effects yields an interesting physical and mathematical problem.

The steady solution of interest is given by

$$\bar{v}_i \equiv 0, \quad \bar{W}_i \equiv 0, \quad \bar{T} = -\beta z + T_L, \quad \bar{C} = -\beta_s z + C_L, \tag{4}$$

where the temperature and concentration gradients, β, β_s, are given by

$$\beta = \frac{T_L - T_U}{d}, \quad \beta_s = \frac{C_L - C_U}{d}.$$

The steady pressure $\bar{p}$ may then be derived up to a constant at ones disposal from $(1)_1$.

To investigate stability of the steady solution (4) we introduce perturbations $(u_i, q_i, \theta, \phi, \pi)$ by

$$v_i = \bar{v}_i + u_i, \quad W_i = \bar{W}_i + q_i, \quad T = \bar{T} + \theta, \quad C = \bar{C} + \phi, \quad p = \bar{p} + \pi.$$

The equations for the perturbations are then derived and non-dimensionalized with the scalings, cf. similar details in section 14.1 of Straughan [49],

$$x_i = x_i^* d, \quad t = t^* \mathcal{T}, \quad U = \frac{\nu}{d}, \quad \mathcal{T} = \frac{d^2}{\nu},$$

$$P = \frac{\rho_0 \nu U}{d}, \quad \epsilon = \frac{\hat{\beta} \mathcal{T}}{\nu} = \frac{\hat{\beta} d^2}{\nu^2} = \frac{\hat{\beta} d}{U \nu}, \quad \lambda = \frac{\hat{\lambda}}{\mathcal{T} \nu} = \frac{\hat{\lambda}}{d^2},$$

$$\gamma = \hat{\gamma} \mathcal{T} = \frac{\hat{\gamma} d^2}{\nu}, \quad T^\sharp = U \sqrt{\frac{\beta \nu}{\kappa g \alpha}}, \quad C^\sharp = U \sqrt{\frac{\beta_s \nu}{\gamma g \kappa_s}}.$$

The Prandtl number, Pr, salt Prandtl number, Pc, the Lewis number, Le, and the Rayleigh and salt Rayleigh numbers, $Ra = R^2$, and $Rs = C^2$, are introduced as

$$Ra = \frac{\alpha g \beta d^4}{\nu \kappa}, \quad Rs = \frac{\beta_s g \gamma d^4}{\kappa_s \nu}, \quad Le = \frac{\kappa}{\kappa_s}, \quad Pr = \frac{\nu}{\kappa}, \quad Pc = \frac{\nu}{\kappa_s}.$$

We next drop the *s and treat x_i and t as the non-dimensional variables. In this manner, we arrive at the following system of non - dimensional perturbation equations arising

from (1),

$$
\begin{aligned}
&u_{i,t} - \lambda \Delta u_{i,t} + u_j u_{i,j} = -\pi_{,i} + \Delta u_i + \epsilon \Delta q_i + R k_i \theta - C \phi k_i, \\
&u_{i,i} = 0, \\
&Pr(\theta_{,t} + u_i \theta_{,i}) = Rw + \Delta \theta, \\
&Pc(\phi_{,t} + u_i \phi_{,i}) = Cw + \Delta \phi, \\
&q_{i,t} + \gamma q_i = u_i,
\end{aligned}
\tag{5}
$$

where $w = u_3$.

Equations (5) are defined on the domain $\mathbb{R}^2 \times \{z \in (0, 1)\} \times \{t > 0\}$ and the boundary conditions are

$$
u_i = 0, \quad q_i = 0, \quad \phi = 0, \quad \theta = 0, \quad z = 0, 1,
\tag{6}
$$

together with the fact that u_i, q_i, ϕ, θ and π satsify a plane tiling periodicity in the x, y plane.

4 Instability Analysis

We commence with an analysis of linear instability for the conduction solution (4). This analysis guarantees a threshold for instability. To initiate the procedure we linearize (5) and seek solutions of the form $u_i = u_i(\mathbf{x})e^{\sigma t}$, $q_i = q_i(\mathbf{x})e^{\sigma t}$, $\phi = \phi(\mathbf{x})e^{\sigma t}$, $\theta = \theta(\mathbf{x})e^{\sigma t}$, $\pi = \pi(\mathbf{x})e^{\sigma t}$. We then remove the pressure term from the equation which arises from (5)$_1$ by taking *curl curl* and retaining the third component. In this way we reduce the system to solving the equations

$$
\begin{aligned}
&\sigma(1 - \lambda \Delta)\Delta w = \Delta^2 w + \epsilon \Delta^2 q_3 + + R \Delta^* \theta - C \Delta^* \phi, \\
&Pr\sigma\theta = Rw + \Delta \theta, \\
&Pc\sigma\phi = Cw + \Delta \phi, \\
&(\sigma + \gamma)q_3 = w,
\end{aligned}
\tag{7}
$$

where $\Delta^* = \partial^2/\partial x^2 + \partial^2/\partial y^2$ is the horizontal Laplacian. Introduce now the forms $q_3 = q_3(z)h(x, y)$, $w = w(z)h(x, y)$, $\theta = \theta(z)h(x, y)$, $\phi = \phi(z)h(x, y)$, where $h(x, y)$ is a planform which reflects the shape of the instability cell, cf. Chandrasekhar [48], pp. 43-52, and $\Delta^* h = -a^2 h$, for a wavenumber a.

The resulting equations hold on the domain $z \in (0, 1)$, and have form

$$
\begin{aligned}
&\sigma(D^2 - a^2)w - \sigma\lambda(D^2 - a^2)^2 w = (D^2 - a^2)^2 w + \epsilon(D^2 - a^2)^2 q_3 \\
&\qquad - a^2 R\theta + Ca^2\phi, \\
&Pr\sigma\theta = Rw + (D^2 - a^2)\theta, \\
&Pc\sigma\phi = Cw + (D^2 - a^2)\phi, \\
&(\sigma + \gamma)q_3 = w,
\end{aligned}
\tag{8}
$$

where $D = d/dz$.

The boundary conditions are

$$w = 0, \quad q_3 = 0, \quad \theta = 0, \quad \phi = 0, \quad \text{on } z = 0, 1. \tag{9}$$

We now consider two stress free surfaces and so we additionally require

$$D^2 w = 0, \quad z = 0, 1. \tag{10}$$

This allows us to write w, q_3, ϕ and θ as a sin series in z of form $\sin(n\pi z)$, $n = 1, 2, \ldots$ We have performed extensive computations and we found $n = 1$ always yields the lowest value of the Rayleigh number. Therefore, we henceforth take $n = 1$ and equations (8) reduce to a 4×4 determinant in w, q_3, θ, ϕ and Λ, where $\Lambda = \pi^2 + a^2$.

After some calculation one shows the Rayleigh number $Ra = R^2$ is given by the expression,

$$R^2 = C^2 \left(\frac{\Lambda + Pr\sigma}{\Lambda + Pc\sigma} \right) + \left[\frac{\sigma \Lambda}{a^2} (1 + \lambda\Lambda) + \frac{\Lambda^2}{a^2} \right] (\Lambda + Pr\sigma) + \epsilon \frac{\Lambda^2}{a^2} \left(\frac{Pr\sigma + \Lambda}{\sigma + \gamma} \right). \tag{11}$$

The stationary convection threshold follows from (11) by taking $\sigma = 0$ and so we find

$$R^2 = C^2 + \frac{\Lambda^3}{a^2} \left(1 + \frac{\epsilon}{\gamma} \right). \tag{12}$$

Upon minimization in a^2 we find the critical wave number value is $a_c^2 = \pi^2/2$ and then the critical stationary convection Rayleigh number is

$$Ra_{stat} = \frac{27\pi^4}{4} \left(1 + \frac{\epsilon}{\gamma} \right) + C^2. \tag{13}$$

To progress we take the real and imaginary parts of (11) and recall that R^2 must be real. To find the oscillatory convection curve we put $\sigma = i\omega$, $\omega \in \mathbb{R}$, and then the real part of (11) yields

$$R^2 = \epsilon \frac{\Lambda^2}{a^2} \left(\frac{\gamma\Lambda + Pr\omega^2}{\gamma^2 + \omega^2} \right) + C^2 \left(\frac{\Lambda^2 + PrPc\,\omega^2}{Pc^2\omega^2 + \Lambda^2} \right) - (1 + \lambda\Lambda)Pr \frac{\Lambda}{a^2}\omega^2 + \frac{\Lambda^3}{a^2} \tag{14}$$

The imaginary part of (11) leads to the equation

$$\frac{\epsilon\Lambda}{a^2} \frac{(\gamma Pr - \Lambda)}{(\gamma^2 + \omega^2)} + \frac{C^2(Pr - Pc)}{(Pc^2\omega^2 + \Lambda^2)} + \frac{\lambda}{a^2} (1 + \lambda\Lambda + Pr) = 0. \tag{15}$$

For equation (15) to hold we require, at least,

$$\Lambda > \gamma Pr \quad \text{or} \quad Pc > Pr, \tag{16}$$

or both conditions to hold simultaneously. Thus, (16) represent necessary conditions for oscillatory convection.

Equation (15) is rearranged to yield a quadratic equation for ω^2, namely,

$$\omega^4 + A\omega^2 + B = 0, \tag{17}$$

where the coefficients A and B are given by

$$A = \frac{\gamma^2 Pc^2 + \Lambda^2}{Pc^2} - \frac{\mathcal{C}^2 a^2 (Pc - Pr)}{Pc^2 \Lambda (1 + \lambda\Lambda + Pr)} - \frac{\epsilon(\Lambda - \gamma Pr)}{(1 + \lambda\Lambda + Pr)}$$

and

$$B = \frac{\gamma^2 \Lambda^2}{Pc^2} - \frac{\mathcal{C}^2 a^2 \gamma^2 (Pc - Pr)}{Pc^2 \Lambda (1 + \lambda\Lambda + Pr)} - \frac{\epsilon \Lambda^2 (\Lambda - \gamma Pr)}{Pc^2 (1 + \lambda\Lambda + Pr)}.$$

The critical values of the oscillatory convection threshold, for R^2, are then found by employing the two solutions, ω_+^2 and ω_-^2, of (17), i.e. $2\omega^2 = -A \pm \sqrt{A^2 - 4B}$, in (14), and minimizing $Ra = R^2$ in a^2 for fixed values of $\lambda, \epsilon, \gamma, Pr$ and Pc, while simultaneously ensuring ω_+^2 and/or ω_-^2 are positive. In fact, for all the values we tried ω_-^2 is always negative.

The fact that $\omega_-^2 < 0$ means that we have not found the interesting neutral curve behaviour where "instability islands" may occur in the $Ra, \mathcal{C}, \epsilon$ space (for fixed γ). The stationary convection curve (13) is a plane in this space (for fixed γ) and it means we do not find closed three dimensional structures underneath the stationary convection plane given by (13), where $\omega_-^2 > 0$ inside, as is found in other areas of multi-component convection, such as double diffusive convection in a rotating fluid, first observed by Pearlstein [60], convection with temperature and two salt fields, Pearlstein et al. [61], penetrative convection with temperature and two salt fields, Straughan and Walker [62], Straughan [49], section 14.2, or inclined convection in a bidisperse porous material, Falsaperla et al. [63].

The neutral curve behaviour obtained from (13), (17) and (14) is a complex relation between $Ra, \mathcal{C}, \epsilon, \gamma, \lambda, Pr$ and Pc, and we report numerical findings in Sect. 6.

5 Global Nonlinear Stability

If one writes the perturbation equations (5) in the form of an abstract equation

$$Au_t = Lu + N(u)$$

where A, L, N are operators mapping into a suitable Hilbert space, where L is the linear operator and $N(u)$ represent the nonlinearities, with

$$u \equiv (u, v, w, q_1, q_2, q_3, \theta, \phi)^T,$$

then concentrating on the part of the linear operator pertaining to the variable $(w, q_3, \theta, \phi)^T$ the essential part of the linear operator has form

$$L_A = \begin{pmatrix} \Delta & \epsilon\Delta & R & -\mathcal{C} \\ -\epsilon\Delta & \Delta & 0 & 0 \\ R & 0 & \Delta & 0 \\ \mathcal{C} & 0 & 0 & \Delta \end{pmatrix}$$

where we have operated first on equation $(5)_5$ by $-\Delta$ and L_A represents the skew symmetric part of L. Upon inspection of L_A there are two skew symmetric effects. One is manifest in the 12 and 21 terms and reflects the presence of the viscoelastic term in $(5)_1$ involving ϵ. In the absence of the salt field this term yields an increasing stability threshold Ra as ϵ increases, and may lead to oscillatory convection, Hopf bifurcation, as shown in figures 2 and 4 of Straughan [64]. The second skew symmetric term in L_A is manifest in the 14 and 41 terms and is due to the fact that the basic layer is heavier in salt at the base. Likewise, without the ϵ term, this salt effect leads to an increase in the Rayleigh number stability threshold as $\mathcal{C}$ increases. It can also lead to oscillatory convection, see Straughan [47], figure 1. Oscillatory convection is increasingly important in multicomponent hydrodynamic systems as is seen in the recent work of Rionero [65], see also Pearlstein [60], Pearlstein et al. [61], Straughan and Walker [62], Falsaperla et al. [63].

In the current problem both skew symmetric effects are present simultaneously and the joint effect is analysed numerically in Sect. 6. However, we may still obtain a global nonlinear stability result by employing the energy functional

$$E(t) = \frac{1}{2}\|\mathbf{u}\|^2 + \frac{\lambda}{2}\|\nabla\mathbf{u}\|^2 + \frac{\epsilon}{2}\|\nabla\mathbf{q}\|^2 + \frac{Pr}{2}\|\theta\|^2 + \frac{Pc}{2}\|\phi\|^2, \qquad (18)$$

where $\|\cdot\|$ denotes the norm on the Hilbert space $L^2(V)$, V being a period cell for the solution. From (5) and (18) one may obtain the energy equation

$$\frac{dE}{dt} = RI - D, \qquad (19)$$

where the production term I, and the dissipation D, have form

$$I(t) = 2(\theta, w),$$
$$D(t) = \|\nabla\mathbf{u}\|^2 + \epsilon\gamma\|\nabla\mathbf{q}\|^2 + \|\nabla\theta\|^2 + \|\nabla\phi\|^2$$

and $(\cdot, \cdot)$ denotes the inner product on $L^2(V)$.

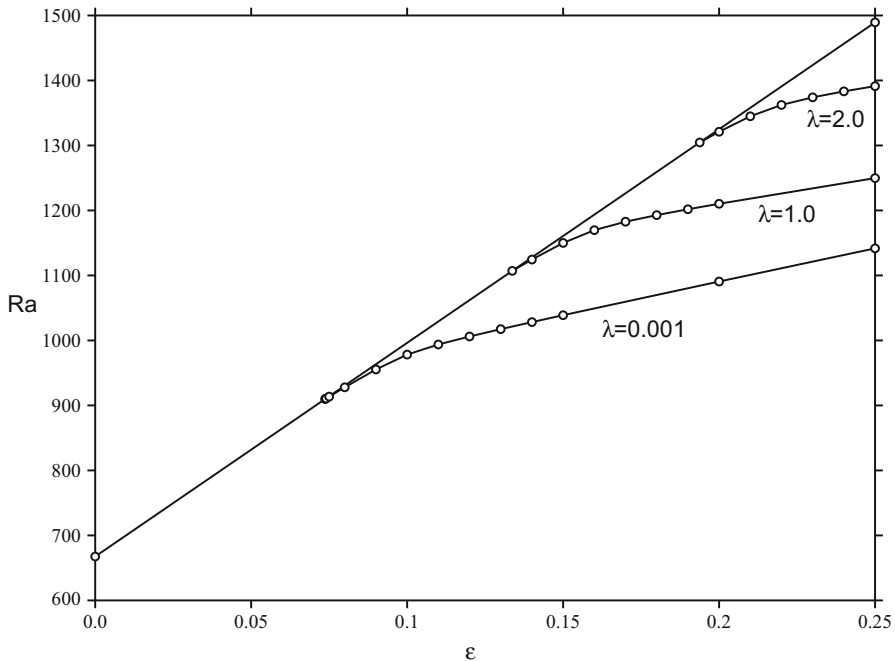**Fig. 1** Graph of Ra, ϵ with $\gamma = 0.2$, $Pr = 25$, $Pc = 541.75$, $\mathcal{C}^2 = 10$. The transition to oscillatory convection is shown for $\lambda = 2$, $\lambda = 1$ and $\lambda = 10^{-3}$. The steady solution is unstable above the appropriate stationary-oscillatory curve. The transition values are approximately $Ra = 909.779$, $\epsilon = 0.0737$ when $\lambda = 10^{-3}$, $Ra = 1107.054$, $\epsilon = 0.1337$ when $\lambda = 1$, and $Ra = 1304.610$, $\epsilon = 0.1938$ when $\lambda = 2$. Kelvin–Voigt fluid of order one

From equation (19) one may show that a global nonlinear energy stability threshold for Ra is given by $Ra \leq 27\pi^4/4$, for two surfaces free of stress. Details are similar to the procedure in Straughan [49], section 14.1. This global stability threshold is depicted in Fig. 5 of this work. We believe it is possible to increase the global stability threshold by employing a generalized energy functional which contains, for example, a term of form $\psi = \theta - \delta\theta$ for a suitable constant $\delta > 0$, cf. Joseph [46], Mulone [39], and possibly a combination of terms involving $u_i, q_i, \nabla u_i, \nabla q_i$. This will undoubtedly involve much analysis and effort employing numerical optimization of coupling parameters with simultaneous minimization in the wavenumber for a generalized energy, cf. Straughan [66], Straughan [41]. This will also require one to involve the Kelvin–Voigt parameter $\lambda > 0$ in a non-trivial manner. This problem of determining the region of possible sub-critical instabilities is currently open.

One thing which is evident from decay of the energy (18) is that for Ra less than the global stability threshold one has decay also of $\|\nabla \mathbf{u}\|$ and $\|\nabla \mathbf{q}\|$, cf. the work of Layton and Rebholz [23], on Kelvin–Voigt vortex solutions, and the numerical computations of Matveeva [28], on a Navier–Stokes–Voigt fluid.
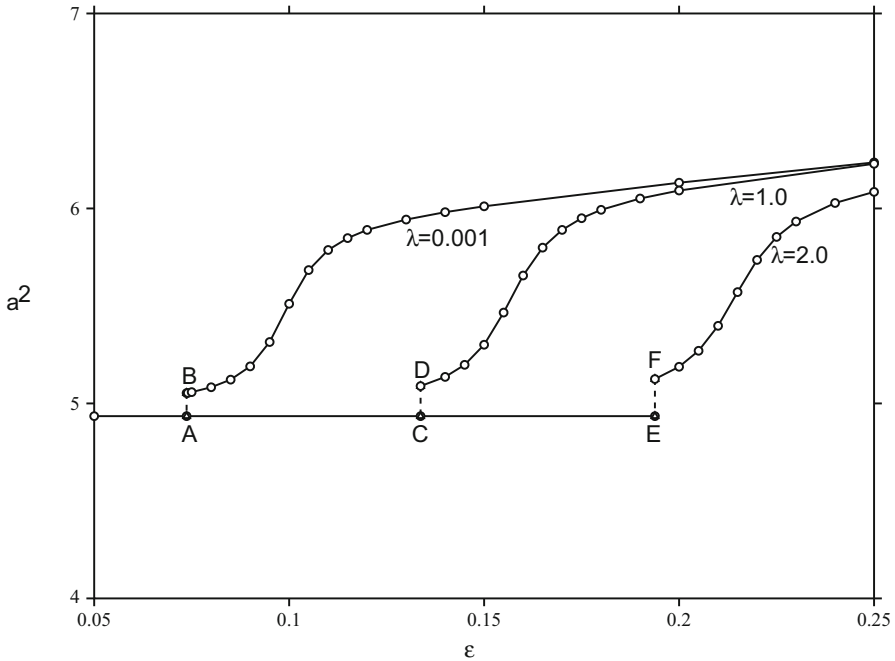
Fig. 2 Graph of a^2, ϵ with $\gamma = 0.2$, $Pr = 25$, $Pc = 541.75$, $\mathcal{C}^2 = 10$. The transition to oscillatory convection is shown for $\lambda = 2$, $\lambda = 1$ and $\lambda = 10^{-3}$. The transition values are approximately $a^2 = 5.053$, $\epsilon = 0.0737$ when $\lambda = 10^{-3}$, see AB, $a^2 = 5.089$, $\epsilon = 0.1337$ when $\lambda = 1$, see CD, $a^2 = 5.125$, $\epsilon = 0.1938$ when $\lambda = 2$, see EF. The stationary convection values of a^2 are $\pi^2/2 \approx 4.9348$. Kelvin–Voigt fluid of order one

6 Numerical Results

In this section we report numerical results based on the stationary convection curve (13) and the results of minimizing (14) with ω^2 given by (17). For the parameters we explore, the values of $\omega^2_{+,-}$ we find are always such that $\omega^2_- < 0$ and we concentrate only on the minimization when $\omega^2_+ > 0$. Figures 1, 2, 3, 4, and 5 and Tables 1, 2, 3, and 4 are based on this strategy.

For fixed $\gamma > 0$, (13) shows the stationary convection surface is a plane in (Ra, Rs, ϵ) space, increasing in Ra as ϵ and Rs increase. For appropriate parameter values oscillatory convection may occur and interest is when the value of Ra, is less than the stationary convection one. The two-dimensional surface of instability for oscillatory convection is found to *not* be a plane in (Ra, Rs, ϵ) space, for fixed γ. When $\epsilon = 0$ oscillatory convection may occur as shown in Straughan [47] and then the oscillatory convection branches appear to be straight lines, see Straughan [47], Fig. 1, with positions depending on λ. When $\mathcal{C} = 0$ oscillatory convection may occur as shown in Straughan [64], Figs. 2 and 4. The oscillatory convection branches again appear to be straight lines which increase in ϵ, and their position depends on λ. However, when $\mathcal{C} \neq 0$ and $\epsilon \neq 0$ we find the situation is more complex.
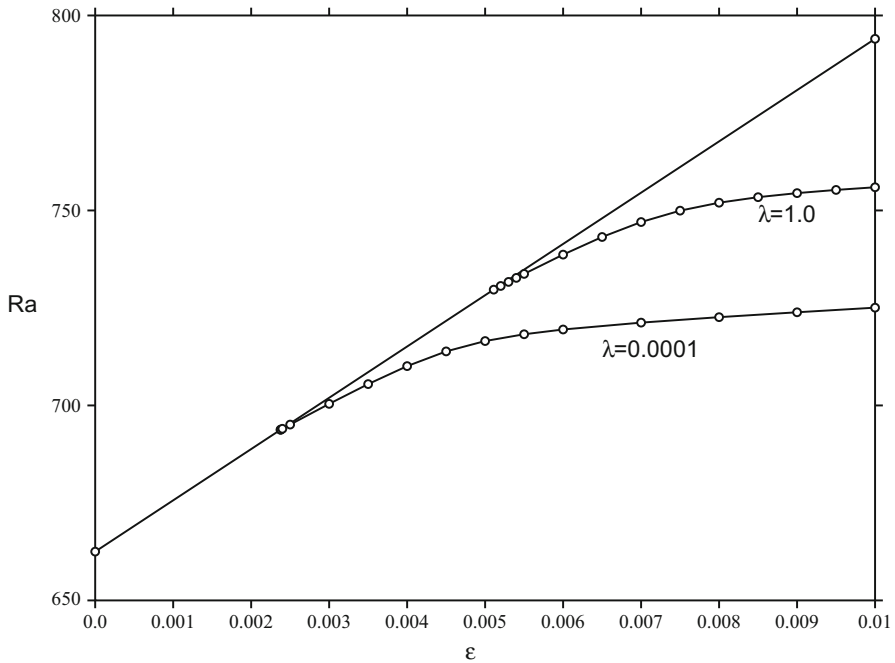
Fig. 3 Graph of Ra, ϵ with $\gamma = 0.05$, $Pr = 25$, $Pc = 1750$, $\mathcal{C}^2 = 5$. The transition to oscillatory convection is shown for $\lambda = 1$ and $\lambda = 10^{-4}$. The steady solution is unstable above the appropriate stationary-oscillatory curve. The transition values are approximately $Ra = 693.753$, $\epsilon = 0.002376$ when $\lambda = 10^{-4}$, and $Ra = 729.694$, $\epsilon = 0.00511$ when $\lambda = 1$. Kelvin–Voigt fluid of order one

We select suitable values of parameters for realistic fluids as in Straughan [47]. To do this recall $Pr = \nu/\kappa$, $Pc = \nu/\kappa_c$ and we note the Lewis number $Le = \kappa/\kappa_c$. In Straughan [47] justification is given for taking Pr in the range 6.99 to 400. Typical values of κ and κ_c given there suggest $\kappa = 1.43 \times 10^{-7}$ m^2 s^{-1}, or in the range

$$4.4 \times 10^{-8} \leq \kappa \leq 8 \times 10^{-8} \ m^2 \ s^{-1,}$$

whereas

$$1.286 \times 10^{-9} \leq \kappa_s \leq 2.03 \times 10^{-9} \ m^2 \ s^{-1}.$$

In Straughan [64] γ is taken as 0.2 or 0.5 and λ values of 10^{-3}, 10^{-2}, 0.1 and 1 are investigated. Given this information we here concentrate on $Pr = 25$, $Pc = 541.75$ or 1750, with λ in the range $[10^{-4}, 2]$.

Figure 1 shows the stationary convection-oscillatory convection branches when $\gamma = 0.2$, $Pr = 25$, $Pc = 541.75$, $\mathcal{C}^2 = 10$, with $\lambda = 10^{-3}$, 1 and 2. We have also computed values for $\lambda = 10^{-2}$ and 0.1, and the trend is in line with that seen here. The transition to oscillatory convection increases in ϵ as λ increases but the oscillatory convection branch is not a straight line. Hence the viscoelastic effect of the parameters ϵ and γ is influencing the critical Rayleigh number values and the
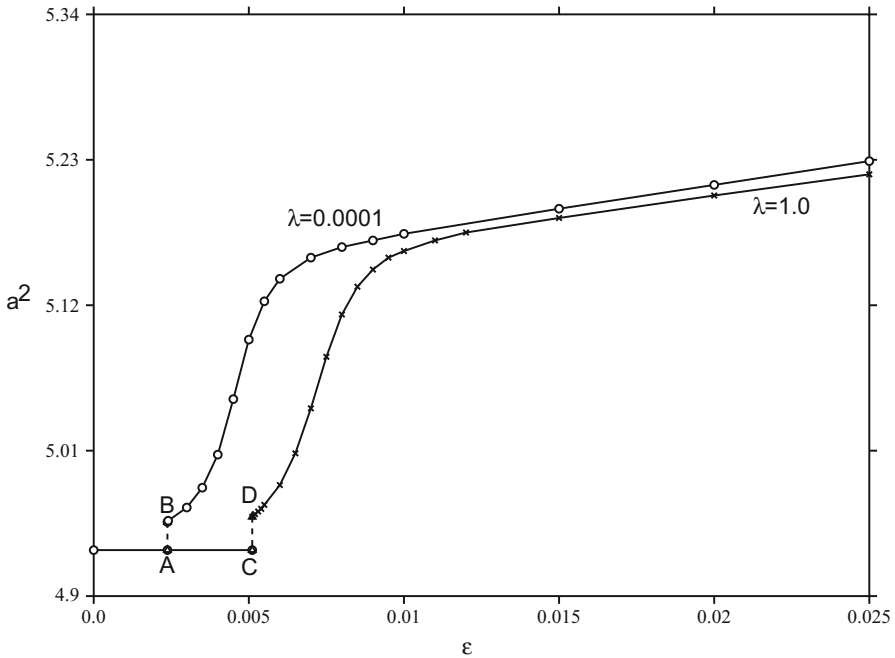
Fig. 4 Graph of a^2, ϵ with $\gamma = 0.05$, $Pr = 25$, $Pc = 1750$, $C^2 = 5$. The transition to oscillatory convection is shown for $\lambda = 1$ and $\lambda = 10^{-4}$. The transition values are approximately $a^2 = 4.956$, $\epsilon = 0.002376$ when $\lambda = 10^{-4}$, see AB, and $a^2 = 4.960$, $\epsilon = 0.00511$ when $\lambda = 1$, see CD. The stationary convection values of a^2 are $\pi^2/2 \approx 4.9348$. Kelvin–Voigt fluid of order one

oscillatory convection surface in (Ra, Rs, ϵ) space is a complex one dependent upon the values of Pr, Pc, Rs, ϵ, γ and λ. The analogous values of the critcal wavenumber are shown in Fig. 2. We see that before the transition to oscillatory convection the stationary convection value of a^2 is always $\pi^2/2$. However, at transition this value jumps discontinuously and thereafter increases with increasing ϵ in a nonlinear way. Since the wavenumber, a, measures the (aspect) ratio of width/depth of a convection cell, larger wavenumber values mean the aspect ratio decreases and one witnesses narrower convection cells. Thus, at transition the cell jumps to a narrower one which then becomes more narrow with increasing ϵ in a nonlinear manner as indicated in Fig. 2.

Figures 3 and 4 show similar transition curves for Ra vs. ϵ and a^2 vs. ϵ when $\gamma = 0.05$, $Pr = 25$, $Pc = 1750$, $C^2 = 5$.

For fixed ϵ but varying C^2 the oscillatory convection curve still has a transition but on the oscillatory convection curve the Ra values increase only very slowly. For example, when $\gamma = 0.05$, $Pr = 25$, $Pc = 1750$, $\epsilon = 0.003$ with $\lambda = 10^{-4}$, the Ra value increases from transition at $C^2 = 9.90034$, where $Ra = 671.357$, to the value $Ra = 672.593$ when $C^2 = 100$. That would indicate that physically the salt field is having a more dominant effect on determining oscillatory convection than the
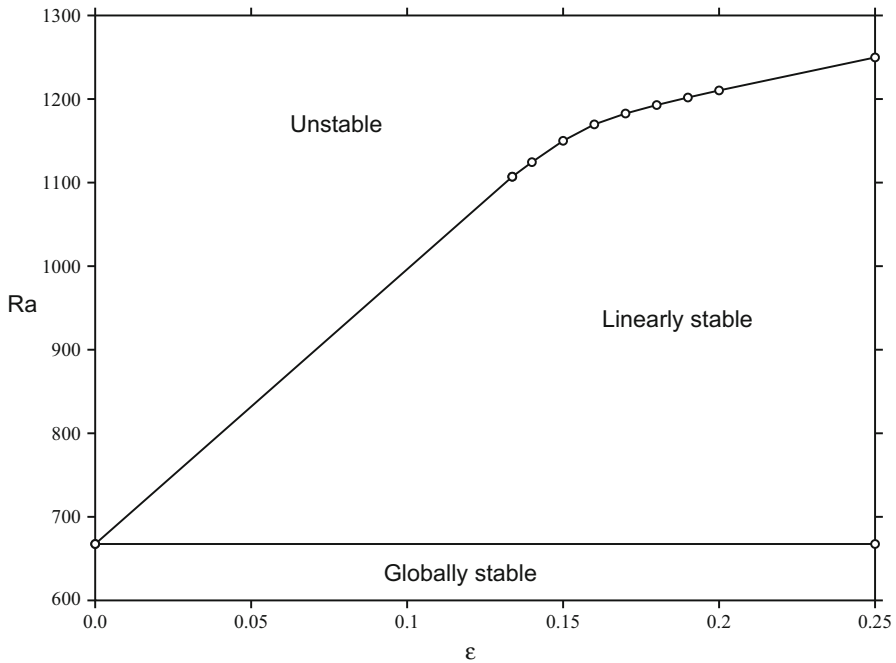
Fig. 5 Graph of Ra, ϵ with $\gamma = 0.2, Pr = 25, Pc = 541.75, C^2 = 10$. The instability and stability regoins are shown for $\lambda = 1$. The transition values are as in Fig. 1. Kelvin–Voigt fluid of order one

Table 1 Transition from stationary to oscillatory convection values, hence $Ra_{osc} = Ra_{stat} \cdot \gamma = 0.2$, $Pr = 25, Pc = 541.75$, $C^2 = 10$. λ varies as shown. Kelvin–Voigt fluid of order one

λ	ϵ	Ra_{osc}	a^2
2	0.1938	1304.610	5.125
1	0.1337	1107.054	5.089
0.1	0.0796	929.197	5.057
0.01	0.0742	911.439	5.053
0.001	0.0737	909.779	5.053

viscoelastic effect of ϵ/γ. The a^2 value over the range just reported stays the same at $a^2 = 4.935$, to 3 d.p.

Table 1 shows the transition to oscillatory convection values when $\gamma = 0.2, Pr = 25, Pc = 541.75, C^2 = 10$, emphasizing the effect of changing λ. It is seen that increasing λ leads to an increase in the equivalent ϵ value, and an increase in a^2, at the transition point.

Table 2 fixes $\gamma = 0.5, Pr = 25, Pc = 1750$ and $\lambda = 1$. The transition to oscillatory convection values are reported as ϵ is increased from 0.6 to 2. The C^2 values decrease as ϵ is increased, with a substantial increase in the values of Ra and a^2. The increase in the Ra values is particularly noticeable and this shows that a large value of ϵ would probably help stabilize the layer.

Table 2 Transition from stationary to oscillatory convection values, hence $Ra_{osc} = Ra_{stat}$

ϵ	Ra_{osc}	a^2	$\mathcal{C}^2$
0.6	1459.97	4.951	13.437
0.8	1722.26	4.953	12.735
1.0	1984.56	4.956	12.028
1.2	2246.86	4.958	11.320
1.4	2509.16	4.961	10.612
1.6	2271.45	4.962	9.904
1.8	3033.75	4.964	9.195
2.0	3296.75	4.965	8.486

$\gamma = 0.5$, $Pr = 25$, $Pc = 1750$, $\lambda = 1$. ϵ varies as shown. Kelvin–Voigt fluid of order one

Table 3 Transition from stationary to oscillatory convection values, hence $Ra_{osc} = Ra_{stat}$

$\mathcal{C}^2$	ϵ	Ra_{osc}	a^2
1	0.01896	783.193	4.992
2	0.01684	770.237	4.974
3	0.01472	757.295	4.967
4	0.01259	744.292	4.961
5	0.01046	731.288	4.956
6	0.00834	718.344	4.952
7	0.00620	705.279	4.948
8	0.00407	692.274	4.949

$\gamma = 0.5$, $Pr = 25$, $Pc = 1750$, $\lambda = 10^{-4}$. $\mathcal{C}^2$ varies as shown. Kelvin–Voigt fluid of order one

Tables 3 and 4 fix $Pr = 25$, $Pc = 1750$, $\lambda = 10^{-4}$ and they employ $\gamma = 0.5$ and $\gamma = 0.05$, respectively. $\mathcal{C}^2$ is increased from 1 to 8 in both tables and the transition values of ϵ, Ra and a^2 are observed. As $\mathcal{C}^2$ increases ϵ decreases, Ra decreases and a^2 decreases in both cases. The instability values of ϵ and Ra are smaller when $\gamma = 0.05$ as opposed to $\gamma = 0.5$. The a^2 values decrease for increasing $\mathcal{C}^2$ but the smaller value of $\gamma = 0.05$ produces a larger range of a^2.

It is clear that the oscillatory convection surface in (Ra, Rs, ϵ) space is dependent on a complicated interaction between the parameters Pr, Pc, γ, $\mathcal{C}^2$ and λ. Once specific values are known for a particular fluid the exact oscillatory instability surface may be calculated.

An important point to observe is that Fig. 5 shows the linear instability transition curve together with the global nonlinear stability one. In Fig. 5, $\mathcal{C}^2 = 10$, but an analogous picture holds for any value of $\mathcal{C}^2$, mutatis mutandis. Given the complicated nature of the linear instability surface, it would be interesting to see nonlinear stability results obtained from a weakly nonlinear analysis, or from three-dimensional numerical simulations.

Table 4 Transition from stationary to oscillatory convection values, hence $Ra_{osc} = Ra_{stat}$

$\mathcal{C}^2$	ϵ	Ra_{osc}	a^2
1	0.00430	715.062	5.003
2	0.00383	709.851	4.980
3	0.00333	704.3	4.993
4	0.00286	699.1	4.962
5	0.00238	693.8	4.956
6	0.00195	689.0	4.953
7	0.00141	683.0	4.947
8	0.00095	678.0	4.943

$\gamma = 0.05$, $Pr = 25$, $Pc = 1750$, $\lambda = 10^{-4}$. $\mathcal{C}^2$ varies as shown. Kelvin–Voigt fluid of order one

7 Conclusions

In this article we develop an analysis for a double diffusive convection problem in a viscoelastic fluid of Kelvin–Voigt order one type. Attention is focussed on the physically interesting and mathematically challenging problem where the layer of fluid is heated from below and simultaneously salted from below. The thermal convection problem for a Navier–Stokes–Voigt fluid without a salt field or for a Kelvin–Voigt fluid of order one without a salt field was suggested by Sukacheva and Matveeva [27], Sukacheva and Kondyukov [29]. An analysis of the thermal convection problem for a Kelvin–Voigt fluid of order one without a salt field is given by Straughan [64], whereas an equivalent analysis of the thermal convection problem for a Navier–Stokes–Voigt fluid is detailed by Straughan [47]. The isothermal models for a Kelvin–Voigt fluid of orders zero, one and higher are explained at length by Oskolkov [25,26], see also Oskolkov and Shadiev [30].

The Kelvin–Voigt fluid of order one contains two extra parameters than the Navier-Stokes–Voigt fluid and these provide a richer structure to the viscoelasticity of the model. From a thermal convection point of view these new effects act like a skew symmetric operator in the instability process, just as the competing effects of heating and salting below act like another, but different, skew symmetric operator. The combination of these two competing effects yields an interesting instability problem which is investigated in some detail in this article.

For small enough Rayleigh number, or small enough viscoelastic parameter ϵ (with γ fixed), the onset of thermally driven motion is by stationary convection. There is then a transition to oscillatory convection as either parameter is increased, or as both are increased. The transition surface is calculated for several realistic values of Prandtl and salt Prandtl numbers. What we see here is that the transition to oscillatory convection occurs at higher Rayleigh numbers as the Kelvin–Voigt parameter λ increases, although the transition values are strongly dependent on the salt Rayleigh number $\mathcal{C}^2 = Rs$.

The increase observed as λ or ϵ increases is very important in real applications. For example, in solar pond design, or in semiconductor crystal growth from a molten liquid. A solar pond is a mechanism whereby solar energy is harnessed through a

thermosolutal process and converted into renewable electric energy, cf. Abdullah et al. [67]. A solar pond consists of a layer of salt water approximately 1–2 m thick in a horizontal configuration with direct access to solar radiation. The salt field is arranged so that the salt concentration decreases approximately linearly from the base of the layer. The base of the layer is chosen to absorb solar radiation and this configuration can achieve temperatures close to 100 °C in the solution near the base. The naturally heated brine solution is drawn out and passed through a heat exchanger to generate renewable electricity. It is important that convective motion does not commence, otherwise the solution mixes and so it is key that the conditions remain in the stable case for the problem studied herein. Our work suggest that adding a suitable additive to the salt solution which increases the Kelvin-Voigt parameter will ensure the solar pond does not commence overturning instability and will, therefore greatly improve the efficiency of the device. In crystal growth, oscillatory convection may lead to striations in the semiconductor crystal which may have a detrimental effect on the ability of the crystal to function in a technical device, see e.g. Jakeman and Hu [68]. Thus an accurate description of the instability surface may help in this field also.

Declarations

Conflict of interest There are no conflicts of interest.

References

1. Haavisto, S., Koponen, A.I., Salmela, J.: New insight into rheology and flow properties of complex fluids with Doppler optical coherence tomography. Front. Chem. **2** (2014). https://doi.org/10.3389/fchem.2014.00027
2. Straughan, B.: Green-Naghdi fluid with non-thermal equilibrium effects. Proc. R. Soc. Lond. A **466**, 2021–2032 (2010)
3. Amendola, G., Fabrizio, M.: Thermal convection in a simple fluid with fading memory. J. Math. Anal. Appl. **366**, 444–459 (2010)
4. Amendola, G., Fabrizio, M., Golden, M., Lazzari, B.: Free energies and asymptotic behaviour for incompressible viscoelastic fluids. Appl. Anal. **88**, 789–805 (2009)
5. Anand, V., Joshua David, J.R., Christov, I.C.: Non-Newtonian fluid structure interactions: static response of a microchannel due to internal flow of a power law fluid. Int. J. Non Newtonian Fluid Mech. **264**, 67–72 (2019)

6. Anand, V., Christov, I.C.: Transient compressible flow in a compliant viscoelastic tube. Phys. Fluids **32**, 112014 (2020)
7. Anand, V., Christov, I.C.: Revisiting steady viscous flow of a generalized Newtonian fluid through a slender elastic tube using shell theory. Z. Angew. Math. Mech. **101**, e201900309 (2021)
8. Anh, C.T., Nguyet, T.M.: Time optimal control of the 3d Navier-Stokes-Voigt equations. Appl. Math. Optim. **79**, 397–426 (2019)
9. Christov, I.C., Christov, C.I.: Stress retardation versus stress relaxation in linear viscoelasticity. Mech. Res. Commun. **72**, 59–63 (2016)
10. Fabrizio, M., Lazzari, B., Nibbi, R.: Aymptotic stability in linear viscoelasticity with supplies. J. Math. Anal. Appl. **427**, 629–645 (2015)
11. Franchi, F., Lazzari, B., Nibbi, R.: Uniqueness and stability results for nonlinear Johnson-Segalman viscoelasticity and related models. Discret. Cont. Dyn. Syst. B **19**, 2111–2132 (2014)
12. Franchi, F., Lazzari, B., Nibbi, R.: Mathematical models for the non-isothermal Johnson-Segalman viscoelasticity in porous media: stability and wave propagation. Math. Methods Appl. Sci. **38**, 4075–4087 (2015a)
13. Franchi, F., Lazzari, B., Nibbi, R.: The Johnson-Segalman model versus a non-ideal MHD theory. Phys. Lett. A **379**, 1431–1436 (2015b)
14. Franchi, F., Lazzari, B., Nibbi, R.: Viscoelastic type magmetic effects and self-gravity on the propagation of MHD waves. Meccanica **55**, 2199–2214 (2020)
15. Gatti, S., Giorgi, C., Pata, V.: Navier-Stokes limit of Jeffreys type flows. Physica D **203**, 55–79 (2005)
16. Jordan, P.M., Puri, A., Boros, G.: On a new exact solution to Stokes' first problem for Maxwell fluids. Int. J. Nonlinear Mech. **39**, 1371–1377 (2004)
17. Jordan, P.M., Puri, A.: Revisiting Stokes' first problem for Maxwell fluids. Q. J. Mech. Appl. Math. **58**, 213–227 (2005)
18. Payne, L.E., Straughan, B.: Convergence for the equations of a Maxwell fluid. Stud. Appl. Math. **103**, 267–278 (1999)
19. Yang, R., Christov, I.C., Griffiths, I.M., Ramon, G.Z.: Time-averaged transport in oscillatory flow of a viscoelastic fluid. Phys. Rev. Fluids **5**, 094501 (2020)
20. Avalos, G.G., Rivera, J.M., Villagram, O.A.: Stability in thermoviscoelasticity with second sound. Appl. Math. Optim. **82**, 135–150 (2020)
21. Chirita, S., Zampoli, V.: On the forward and backward in time problems in the Kelvin-Voigt thermoelastic materials. Mech. Res. Commun. **68**, 25–30 (2015)
22. El Arwadi, T., Youssef, W.: On the stabilization of the Bresse beam with Kelvin–Voigt damping. Appl. Math. Optim. **83** (2021). https://doi.org/10.1007/s00245-019-09611-z
23. Layton, W.J., Rebholz, L.G.: On relaxation times in the Navier–Stokes–Voigt model. Int. J. Comput. Fluid Dyn. **27**, 184–187 (2013)
24. Rivera, J.M., Racke, R.: Transmission problems in (thermo) viscoelasticity with Kelvin–Voigt damping: non-exponential, strong and polynomial stability. SIAM J. Math. Anal. **49**, 3741–3765 (2017)
25. Oskolkov, A.P.: Initial-boundary value problems for the equations of Kelvin–Voigt fluids and Oldroyd fluids. Proc. Steklov Inst. Math. **179**, 126–164 (1988)
26. Oskolkov, A.P.: Nonlocal problems for the equations of motion of Kelvin-Voigt fluids. J. Math. Sci. **75**, 2058–2078 (1995)
27. Sukacheva, T.G., Matveeva, O.P.: On a homogeneous model of the non-compressible viscoelastic Kelvin–Voigt fluid of the non-zero order. J. Samara State Tech. Univ. Ser. Phys. Math. Sci. **5**, 33–41 (2010)
28. Matveeva, O.P.: Model of thermoconvection of incompressible viscoelastic fluid of non-zero order-computational experiment. Bull. South Ural State Tech. Univ., Ser. Math. Model. Program. **6**, 134–138 (2013)
29. Sukacheva, T.G., Kondyukov, A.O.: On a class of Sobolev type equations. Bull. South Ural State Tech. Univ., Ser. Math. Model. Program. **7**, 5–21 (2014)
30. Oskolkov, A.P., Shadiev, R.: Towards a theory of global solvability on $[0, \infty)$ of initial-boundary value problems for the equations of motion of Oldroyd and Kelvin - Voigt fluids. J. Math. Sci. **68**, 240–253 (1994)
31. Christov, I.C., Jordan, P.M.: Maxwell's "other" equations. Blog, The Royal Society (2015). https://royalsociety.org/blog/2015/09/maxwells-other-equations
32. Barletta, A., Nield, D.A.: Thermosolutal convective instability and viscous dissipation effect in a fluid-saturated porous medium. Int. J. Heat Mass Transf. **54**, 1641–1648 (2011)

33. Capone, F., Gentile, M., Hill, A.A.: Double diffusive penetrative convection simulated via internal heating in an anisotropic porous layer with throughflow. Int. J. Heat Mass Transf **54**, 1622–1626 (2011)
34. Galdi, G.P., Payne, L.E., Proctor, M.R.E., Straughan, B.: Convection in thawing subsea permafrost. Proc. R. Soc. Lond. A **414**, 83–102 (1987)
35. Gentile, M., Straughan, B.: Hyperbolic diffusion with Christov–Morro theory. Math. Comput. Simul. **127**, 94–100 (2016)
36. Harfash, A.J., Hill, A.A.: Simulation of three dimensional double diffusive throughflow in internally heated anisotropic porous media. Int. J. Heat Mass Transf. **72**, 609–615 (2014)
37. Nield, D.A.: The thermohaline Rayleigh–Jeffreys problem. J. Fluid Mech. **29**, 545–558 (1967)
38. Matta, A., Narayana, P., Hill, A.A.: Double diffusive Hadley–Prats flow in a horizontal layer with a concentration based internal heat source. J. Math. Anal. Appl. **452**, 1005–1018 (2017)
39. Mulone, G.: On the nonlinear stability of a fluid layer of a mixture heated and salted from below. Continuum Mech. Thermodyn. **6**, 161–184 (1994)
40. Payne, L.E., Song, J.C., Straughan, B.: Double diffusive penetrative convection: thawing subsea permafrost. Int. J. Eng. Sci. **103**, 797–809 (1999)
41. Straughan, B.: Tipping points in Cattaneo-Christov thermohaline convection. Proc. R. Soc. Lond. A **467**, 7–18 (2011)
42. Straughan, B.: Anisotropic inertia effect in microfluidic porous thermosolutal convection. Microfluidics Nanofluidics **16**, 361–368 (2014)
43. Straughan, B.: Heated and salted below porous convection with generalized temperature and solute boundary conditions. Trans. Porous Media **131**, 617–631 (2020)
44. Straughan, B.: Convection with Local Thermal Non-equilibrium and Microfluidic Effects, vol. 32 of Advances in Mechanics and Mathematics Series. Springer, Cham (2015)
45. Straughan, B., Hutter, K.: A priori bounds and structural stability for double diffusive convection incorporating the Soret effect. Proc. R. Soc. Lond A **455**, 767–777 (1999)
46. Joseph, D.D.: Global stability of the conduction diffusion solution. Arch. Ration. Mech. Anal. **36**, 285–292 (1970)
47. Straughan, B.: Thermosolutal convection with a Navier–Stokes–Voigt fluid. Appl. Math. Optim. **83** (2021). https://doi.org/10.1007/s00245-020-09719-7
48. Chandrasekhar, S.: Hydrodynamic and Hydromagnetic Stability. Dover, New York (1981)
49. Straughan, B.: The Energy Method, Stability, and Nonlinear Convection, 2nd edn, vol. 91 of Appl. Math. Sci. Springer, New York (2004)
50. Greco, R., Marano, G.C.: Identification of parameters of Maxwell and Kelvin–Voigt generalized models for fluid viscous dampers. J. Vib. Control **21**, 260–274 (2015)
51. Christov, C.I.: On frame indifferent formulation of the Maxwell-Cattaneo model of finite-speed heat conduction. Mech. Res. Commun. **36**, 481–486 (2009)
52. Jordan, P.M., Passerella, F., Tibullo, V.: Poroacoustic waves under a mixture—theoretic based reformulation of the Jordan-Darcy-Cattaneo model. Wave Motion **71**, 82–92 (2017)
53. Gidde, R.R., Pawar, P.M.: On the effect of viscoelastic characterizations on polymers and on performance of micropump. Adv. Mech. Eng. **9**, 1–12 (2017)
54. Jayabal, H., Dingari, N.N., Rai, B.: A linear viscoelastic model to understand the skin mechanical behaviour and for cosmetic formulation design. Int. J. Cosmetic Sci. **41**, 292–299 (2019)
55. Jozwiak, B., Orczykowska, M., Dziubinski, M.: Fractional generalizations of Maxwell and Kelvin–Voigt models for biopolymer characterization. PLoS ONE **15** (2015). https://doi.org/10.1371/journal.pone.0143090
56. Erdel, F., Baum, M., Rippe, K.: The viscoelastic properties of chromatin and the nucleoplasm revealed by scale-dependent protein mobility. J. Phys. **27**, 064115 (2015)
57. Askarian, A.R., Permoon, M.R., Shakouri, M.: Vibration analysis of pipes conveying fluid resting on a fractional Kelvin-Voigt viscoelastic foundation with general boundary conditions. Int. J. Mech. Sci. **179** (2020). https://doi.org/10.1016/j.ijmecsci.2020.105702
58. Lewandowski, R., Chorazyczewski, B.: Identification of the parameters of the Kelvin–Voigt and the Maxwell models, used to modelling viscoelastic dampers. Comput. Struct. **88**, 1–17 (2010)
59. Xu, Z.D., Wang, D.X., Shi, C.F.: Model, tests and application design for viscous dampers. J. Vib. Control **17**, 1359–1370 (2010)
60. Pearlstein, A.J.: Effect of rotation on the stability of a doubly diffusive fluid layer. J. Fluid Mech. **103**, 389–412 (1981)

61. Pearlstein, A.J., Harris, R.M., Terrones, G.: The onset of convective instability in a triply diffusive fluid layer. J. Fluid Mech. **202**, 443–465 (1989)
62. Straughan, B., Walker, D.W.: Multi-component diffusion and penetrative convection. Fluid Dyn. Res. **19**, 77–89 (1997)
63. Falsaperla, P., Mulone, G., Straughan, B.: Bidispersive inclined convection. Proc. R. Soc. Lond. A **472**, 20160480 (2016)
64. Straughan, B.: Instability thresholds for thermal convection in a Kelvin–Voigt fluid of variable order. Rend. Circ. Matem. Palermo **70** (2021). https://doi.org/10.1007/s12215-020-00588-1
65. Rionero, S.: Hopf bifurcations in quaternary dynamical systems of rotating thermofluid mixtures, driven by spectrum characteristics. Ricerche di Matem. **70** (2021). https://doi.org/10.1007/s11587-020-00514-8
66. Straughan, B.: Global stability for convection induced by absorption of radiation. Dyn. Atmos. Oceans **35**, 351–361 (2002)
67. Abdullah, A.A., Fallatah, H.M., Lindsay, K.A., Oreijah, M.M.: Measurements of the performance of the experimental salt-gradient solar pond at Makkah one year after commissioning. Solar Energy **150**, 212–219 (2017)
68. Jakeman, E., Hurle, D.T.J.: Thermal oscillations and their effect on solidification processes. Rev. Phys. Technol. **3**, 3–30 (1972)